

~~NRC~~  
NRC

***NTS SYSTEMS MODEL***

PREPARED BY

PETER ORNSTEIN

MICHAEL WEBER

JANUARY, 1983

HYDROLOGY DOCUMENT NUMBER 221

PERFORMANCE ASSESSMENT SECTION  
HIGH LEVEL WASTE LICENSING MANAGEMENT BRANCH  
U.S. NUCLEAR REGULATORY COMMISSION

Document Name:  
3102/PMO/83/01/10/0

Requestor's ID:  
MIKEW

Author's Name:  
PMOrnstein

Document Comments:  
OPS Plan Commitment, DUE 1/28/83, re: NTS

## INTRODUCTION

The Nevada Test Site in southern Nevada has been selected by the Department of Energy as a primary candidate for a HLW repository. Since the NRC has the regulatory responsibility of insuring that such facilities will meet the requisite EPA safety standards, the NRC needs to be able to evaluate the repository performance well into the future. Due to the complexities of the processes involved in radionuclide release and migration, computer codes are required to solve the differential equations that are used to describe groundwater flow and radionuclide transport away from the repository.

This document will present a methodology which makes use of NRC computer codes to model groundwater flow in the vicinity of, and potential radionuclide transport away from, a HLW repository at the Nevada Test Site. Although the methodology will be used to study radionuclide migration in both the saturated and unsaturated zones, this paper will focus primarily on the unsaturated zone.

As of this writing, the anticipated repository location at NTS will be in the unsaturated tuffs beneath Yucca Mountain. The physical processes and parameters governing groundwater flow and transport in the unsaturated zone are very complex and not readily definable. Compounding these uncertainties are the heat induced effects caused by the repository's thermal loading. In order to numerically model flow in the unsaturated zone, many simplifying assumptions need to be made in the interpretation of available data so as to bring the modeling capabilities of the computer codes in line with the degree of knowledge of the input

parameters. Characterization of the unsaturated flow parameters is currently an area of major uncertainty.

### CONCEPTUAL MODELS

Prior to application of computer codes and as an initial phase in the proposed methodology, conceptual models of the geology and groundwater flow system need to be developed. These conceptualizations should encompass a wide range of both likely and unlikely flow scenarios so as to bound and include the real flow regime. Development of these conceptualizations will serve as a basis for formulating the computer model input parameters.

The scenarios that follow were designed to address extremes in geologic and thermal conditions that might significantly affect radionuclide travel times. Further evaluation of some of these scenarios may show them to be physically impossible; however for completeness they will be included and discussed. Most of the scenarios are applicable to hot (repository temperature > ambient temperature) or cold (repository temperature ~ ambient temperature) conditions even though flow paths may vary significantly between the two.

### Discussion Of Scenarios

The scenarios depicted and described in the following section are presented without an evaluation of their probability of occurrence. While several of these scenarios are more plausible than the others, the complete pre-placement performance assessment of a potential HLW

repository must evaluate a full range of release or failure modes. The results of such a sensitivity analysis must then be resolved in light of the probabilities of scenario occurrence. This approach is particularly applicable in the conceptual modeling of groundwater flow and transport at Yucca Mountain. Since so little is known about groundwater migration and radionuclide transport through variably-saturated fractured porous media compared to conventional isotropic homogeneous darcy flow through saturated media, these scenarios or conceptual models must bound travel times and contaminant transport to the accessible environment.

As the water percolates through the unsaturated zone, it encounters three generalized hydrostratigraphic rock types: vitric air fall tuffs, zeolitized tuffs, and welded flow tuffs. These rock types differ mechanically, hydraulically, and petrologically. Air fall tuffs are pyroclastic rocks that form from volcanic dust, ash, lapilli, bombs, and blocks which are projected from the volcanic vent into the troposphere. As they fall back to the earth's surface, they accumulate as poorly-consolidated blankets of ash that mantle the topography surrounding the volcano. Though many of the air fall tuffs at NTS formed subaerially, resedimented tuffs may have formed as ash accumulated in playa lakes or as earlier tuffs eroded to supply sediment to alluvial streams and fans. Air fall tuffs, when composed of glass shards, are called vitric. Similarly, lithic air fall tuffs are predominantly composed of rock fragments, and crystalline fall tuffs are comprised of crystals that formed within the magma reservoir and vented during the eruption. Air fall tuffs are typically well-stratified and decrease systematically in average grain size and bed thickness away from the source vent. Normal or reverse vertical grading, however, cannot be used as a genetic indicator since it is largely a function of the eruptive intensity which may change during any single volcanic event. As many air

fall tuffs are poorly- to non-welded, depending upon the temperature of the ash as it accumulates, they are structurally incompetent, and therefore, air fall tuffs cannot support open fractures. Percolating groundwater probably flows through tortuous paths of interconnected pores approximating darcy flow. As the tuffs are generally highly porous and the water flows through the pores, the contacted surface area is very large, which improves the chances of radionuclide sorption onto the reactive glass shards, clays, or zeolites. The transmissivities of the air fall tuffs may vary considerably due to spatial variation in thicknesses and the extent of zeolitic or argillic alteration. Hydraulic conductivities and porosities may vary significantly due to extreme heterogeneities, while at any given spot the unit may be isotropically conductive. Laboratory porosities for the Claim Canyon Tuff vary from 5 to 50 % on the scale of several feet. The hydraulic properties will remain unpredictable until a valid genetic model is developed which can be applied generically to fall tuffs at any location. This unpredictability complicates predictive modeling of the Yucca Mountain site.

Where the air fall or flow tuffs have been extensively argillitized or zeolitized, the hydraulic properties differ from those of the air fall or flow tuffs. These units are characterized as zeolitized tuffs. Secondary mineralization increases the consolidation of the tuff to make it more competent and prone to brittle fracture. While the hydraulic conductivity and porosity of the matrix are reduced compared to those of the air fall tuffs, open fractures increase the secondary porosity to augment the primary porosity. Percolating water in the vadose zone may be rapidly transmitted along the fractures without the beneficial sorption of ions that would take place within the rock matrix.

Unlike the air fall tuffs which accumulate as ash, dust, and lapilli fall from the atmosphere, welded flow tuffs form where superheated gases entrain and transport the volcanic particulates away from the volcano. During sicilian-type eruptions of alkalic and silicic magmas, viscous and gaseous lava streams down the flanks of the volcano at temperatures between 700 and 1000 ° C and velocities from 10s to 100s of kilometers per hour. Glass shards, which form as the rapidly expanding gas vessicles explode, weld together in the intense heat of the flow. Portions of the flow which are cooler than the interior may weld less completely than the core of the flow. Thus, the degree of welding varies vertically and laterally within the flow unit. In addition, the hydraulic regime during the period of flow deposition will control the primary structures, distribution of lithophysae, and the abundance of gas vessicles, blocks, and bombs within the flow unit. Figure illustrates the primary structures which are commonly present in subaerial ash flow tuffs.

Water that enters the moderately- to densely-welded flow tuffs is conducted primarily along fractures. Comprised mostly of welded glass, flow tuffs are characteristically more brittle than air fall or zeolitized tuffs; they are more competent and can easily support open fractures. In addition to transmission along fractures, interconnected lithophysal cavities provide alternate pathways for the water to percolate through the flow tuffs. Welded flow tuffs have extremely low intercrystalline porosities and hydraulic conductivities.

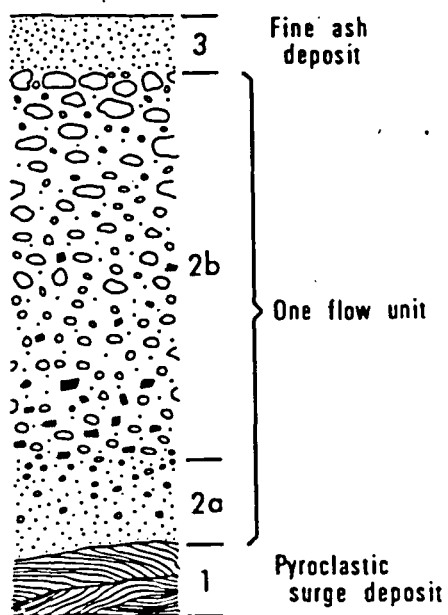


Figure 3. Primary flow structures within a generic pyroclastic flow unit (Lajourie, 1980).

Within the unsaturated zone, water in the rock matrix is held in tension (i.e. negative matric or pressure potential) as moisture contents are below saturation. Open fractures, however, may be saturated several hundred feet above the regional water table. When they are penetrated, (i.e. by a well bore or during shaft excavation) many of the fractures will drain with flow decreasing exponentially with time. Since these flows are unique events and the fractures have not been observed to resaturate, it is believed that the fractures essentially pond the water because they are not interconnected. Other fractures, however, continue to seep water during an observation period of several months. This may indicate that some fractures are indeed interconnected and are being recharged with infiltration from other fractures within the welded tuffs from above. Water seeping from fractures near Rainier Mesa contain possible post-bomb tritium. Relatively rapid transport of tritium in several decades through thousands of feet of tuff is required if the tritium observed is post-bomb tritium. Thus, percolating water may be conducted with relatively high velocities through the fractures and interconnected lithophysal cavities of the welded tuffs.

Transmissivities of the welded tuffs are controlled by densities, apertures, geometries, and persistences of fractures and thicknesses of the individual flow units. Since ash flows accumulate in the topographically low areas around the volcanic vent, their transmissivity will vary spatially as a function of flow thickness in response to the original surface morphology. Fractures develop within the brittle tuffs in response to devitrification and vapor-phase crystallization stresses, tension and compression during cooling, expansion and contraction during zeolitization and argillitization, and tectonic tension and compression. Highly-fractured, densely welded tuffs may have hydraulic conductivities which are five to six orders of magnitude higher than the intergranular conductivities ( $10E-3$  versus  $10E-9$  cm/s). Fracture orientations control the anisotropy of the hydraulic conductivity within the welded tuffs.

Fractures may also be important as highly conductive conduits between the intercalated zeolitized and air fall tuffs. As with the air fall tuffs, a genetic model incorporating all of these stresses, strains, and the flow controls by fractures within the welded tuffs would be necessary to predict the spatial variation in transmissivity of the moderately- to densely-welded tuffs at NTS. Without such a model, the system must be characterized by in-situ tests, for laboratory analyses of porosity and hydraulic conductivity of fractured rocks are of questionable value.

Porosity may also vary as a function of the degree of welding within the flow unit. The glass shards that comprise the flow tuff weld the greatest in the hottest portions of the flow. As the degree of welding increases, the average grain density increases while the intergranular porosity decreases. Because the hydraulic conductivity and porosity depend upon the genetic history of the flow unit, they may vary considerably within a single flow unit or series of flow units.

#### SCENARIO I: Normal Infiltration

In this model, precipitation that falls on the land surface above the repository infiltrates the unsaturated tuffs, percolates vertically downward, and enters the saturated flow system at the regional water table several hundred feet below the repository horizon. As in all of these scenarios, the repository is located within the densely-welded Topopah Springs Member at the base of the Paintbrush Tuff Formation (see Figure 2). Percolating water is driven through the unsaturated zone by gravity, and the thermal effects of the repository are considered nominal. Within the unsaturated zone, matric potentials or pressure heads are strongly negative (tension), but because the elevation heads

EPOCH	ERUPTIVE CENTER	FORMATION	MEMBERS OR RELATED UNITS	RADIOMETRIC AGE-10 <sup>6</sup> YRS	ESTIMATED VOLUME-MI <sup>3</sup>
PLIOCENE	BLACK MOUNTAIN CALDERA	THIRSTY CANYON TUFF	LABYRINTH CANYON MEMBER GOLD FLAT MEMBER TRAIL RIDGE MEMBER SPEARHEAD MEMBER ROCKET WASH MEMBER	6-8	50
	TIMBER MOUNTAIN CALDERA	TIMBER MOUNTAIN TUFF	RHYOLITES OF SHOSHONE MOUNTAIN MAFIC LAVAS OF DOME MOUNTAIN RHYOLITES OF FORTY MILE CANYON TUFFS OF CROOKED CANYON AND BUTTONHOOK WASH AMMONIA TANKS MEMBER RAINIER MESA MEMBER	9.5-11.5	? BUT SMALL ? BUT SMALL ? BUT SMALL 230 300
MIOCENE	WAHMONIE - MT. SALYER AREA	WAHMONIE FORMATION SALYER FORMATION	MULTIPLE RHYOLITE, ANDESITE AND BRECCIA FLOWS, AND THIN TUFFS	12-13	50?
	CLAIM CANYON CALDERA - CALICO HILLS	PAINTBRUSH TUFF	RHYOLITE FLOWS TIVA CANYON MEMBER YUCCA MOUNTAIN MEMBER LAVA FLOWS PAH CANYON MEMBER TOPOPAH SPRINGS MEMBER	12-13	? 250 4 ? 5 60
		CALICO HILLS FORMATION	RHYOLITES OF CALICO HILLS ASHFLOW AND ASHFALL TUFFS	13-14	?
	SILENT CANYON CALDERA	STOCKADE WASH TUFF		13-15	5-10
		BELTED RANGE TUFF	GROUSE CANYON MEMBER TUB SPRINGS MEMBER	13-15	75
	CRATER FLAT AREA - SLEEPING BUTTE CALDERA	CRATER FLAT TUFF	PROW PASS MEMBER BULLFROG MEMBER TRAM MEMBER	14-15	300
		PED ROCK VALLEY TUFF		14-16	? BUT SMALL
	MT HELEN	TOLICHA PEAK TUFF	MULTIPLE COOLING UNITS	>14	?
	KANE SPRINGS WASH CALDERA	KANE WASH TUFF	MULTIPLE COOLING UNITS LAVA FLOWS	14-15	200
	CACTUS - KAWICH RANGES	RHYOLITE LAVA FLOWS	O'BRIEN'S KNOB, CACTUS PEAK BELTED PEAK, OCHER RIDGE	14-15	200
	CATHEDRAL RIDGE CALDERA	FRACTION TUFF	MULTIPLE COOLING UNITS	15-18	500
	MT. HELEN, CACTUS - KAWICH RANGES	FLOWS OF INTERMEDIATE COMPOSITION	DACITES, ANDESITES, QUARTZ LATITES	18-22	?
		WHITE BLOTCH SPRING TUFF	MULTIPLE COOLING UNITS	24-25	500
OLI-GOCENE		ANTELOPE VALLEY TUFF	MULTIPLE COOLING UNITS	26-27	?
	PANCAKE RANGE	MONOTONY TUFF	MULTIPLE COOLING UNITS	26-28	1000

Figure 2. Simplified volcanic stratigraphy of NTS (Sinnock, 1982, p.33).

are larger in magnitude and positive, the total head is also positive and decreases downward. Figure 2 illustrates the changes in pressure and total heads with increasing depth. At the water table, total head equals the elevation head, which is the height of the water table above the regional base level.

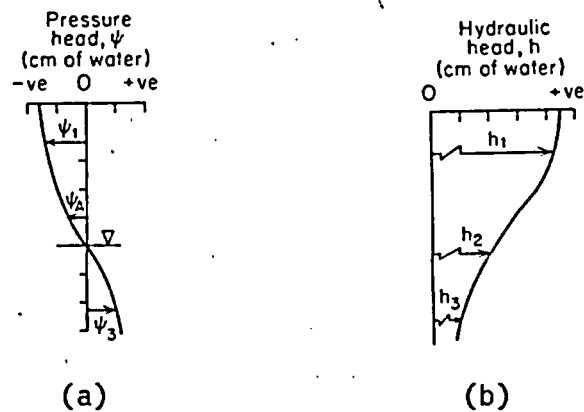
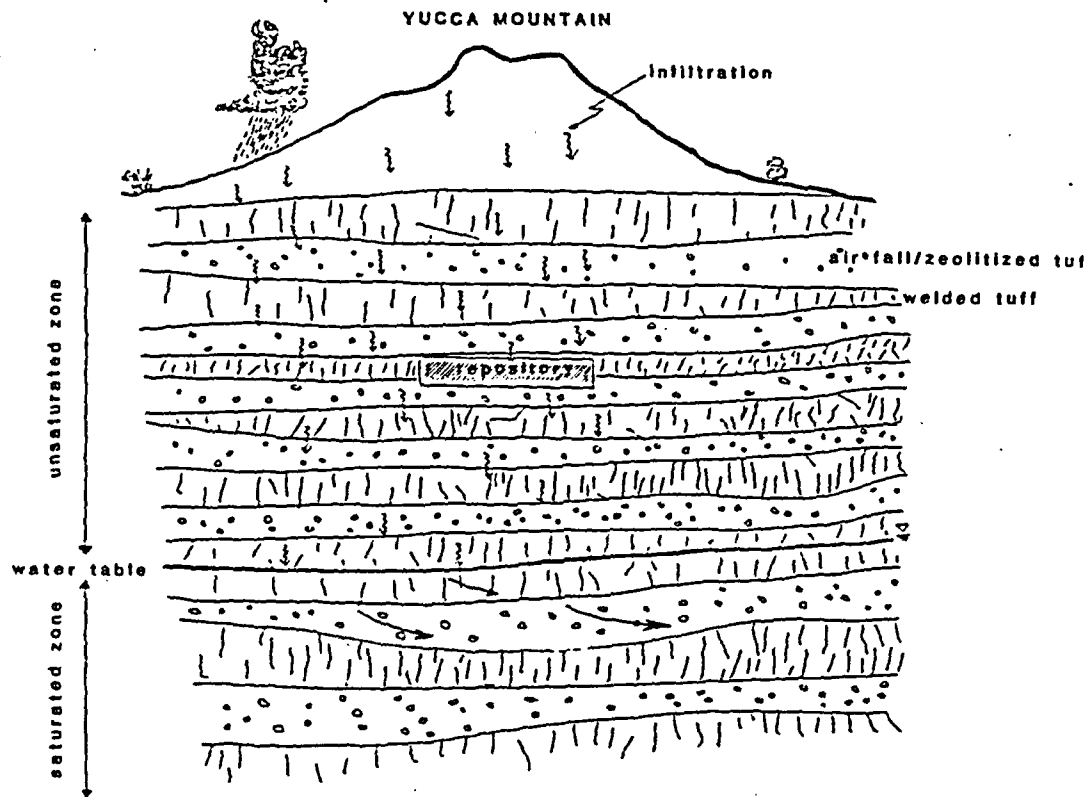


Figure 3. Pressure head (a) and hydraulic head (b) as a function of depth below surface ( Freeze and Cherry, 1979, p. 40).

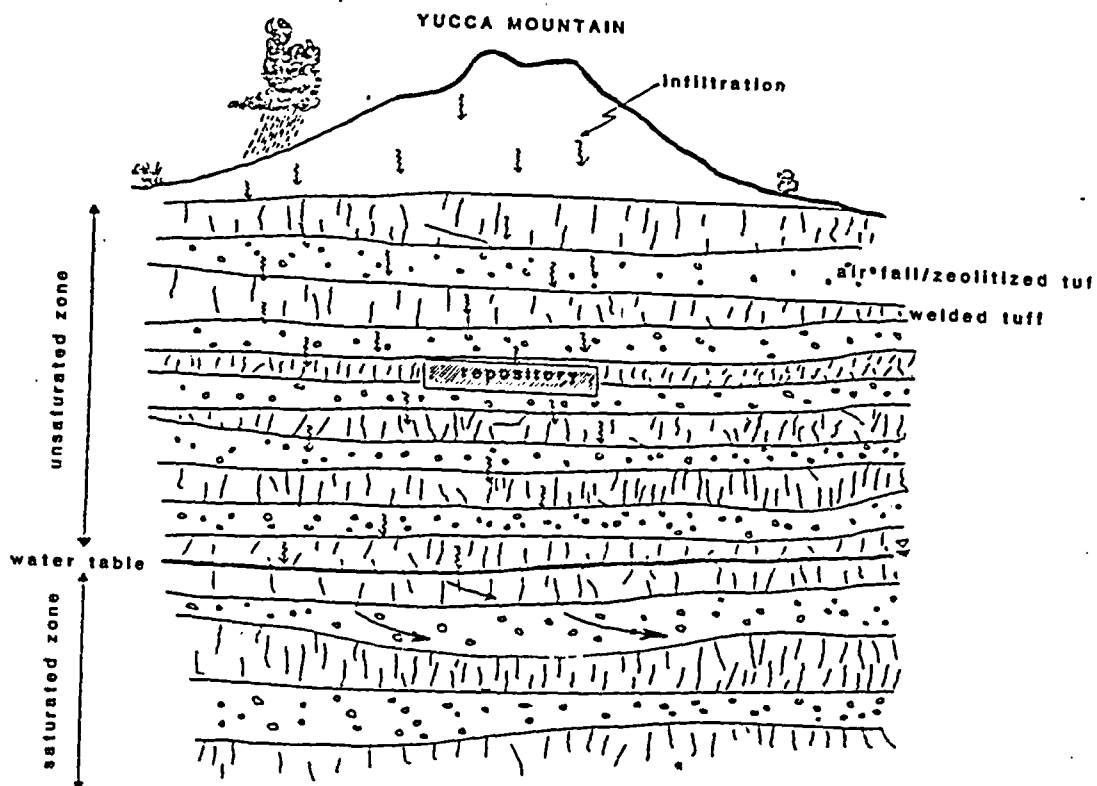
The alternating layers of air fall, zeolitized, and welded flow tuffs at Yucca Mountain may be an effective barrier against rapid groundwater flow through the unsaturated zone. In this scenario, pictured in Figure 4, lateral disparities in porosities and conductivities are eliminated by the assumption of unidirectional flow. This flow begins at the surface, where precipitation that escapes runoff and evaporation infiltrates into the upper portion of the unsaturated zone. Although precipitation at Yucca Mountain averages about 5 to 6 cm annually, regional groundwater modeling studies and water budget calculations indicate that only 10 % actually recharges the saturated zone, which is several hundred meters below the surface. These estimates should be refined by tests within the vadose zone at NTS by DOE. Precipitation could increase significantly during a period of pluviation, similar to that which occurred during the Late Wisconsinan Glacial Stage. This increased precipitation would not necessarily increase infiltration if the unsaturated vitric air fall tuffs above the Topopah Springs Member behave as vadose water wicks; by absorbing the differential infiltration, these units would increase their saturation and delay the transmission of the infiltration to the lower vadose zone.



### NTS RELEASE SCENARIO

Figure 4. Diagram of NTS Infiltration Scenario.

In this scenario, 3 mm of water infiltrates the upper vadose zone; percolates through the zeolitized, air fall, and welded flow tuffs; and intercepts the repository before reaching the regional water table. After it leaves the repository, it flows downward until it intercepts the water table where it enters the phreatic or saturated zone. Once in the phreatic system, it flows in response to regional hydraulic gradients, and radionuclides that were leached from the waste are transported towards the accessible environment.



### NTS RELEASE SCENARIO

Figure 4. Diagram of NTS Infiltration Scenario.

In this scenario, 3 mm of water infiltrates the upper vadose zone; percolates through the zeolitized, air fall, and welded flow tuffs; and intercepts the repository before reaching the regional water table. After it leaves the repository, it flows downward until it intercepts the water table where it enters the phreatic or saturated zone. Once in the phreatic system, it flows in response to regional hydraulic gradients, and radionuclides that were leached from the waste are transported towards the accessible environment.

## SCENARIO II: FINGERING

The vitric air fall and zeolitized tuffs may saturate above the repository, particularly if recharge increases during pluviation. Since the intercalated welded tuffs are more transmissive than the less-fractured tuffs, water may perch above and within the units of higher intergranular porosities and lower effective conductivities. Perched water may eventually percolate through the more porous layers by fingering, a process where water is conducted rapidly through a porous media along macropores may be present within poorly consolidated materials. Fingering is commonly observed within soils and has been recognized as an effective and rapid transport process introducing bacteria, pesticides, and hazardous wastes to the deeper flow system faster than would be expected with darcy flow (Simpson and Cunningham, 1982).

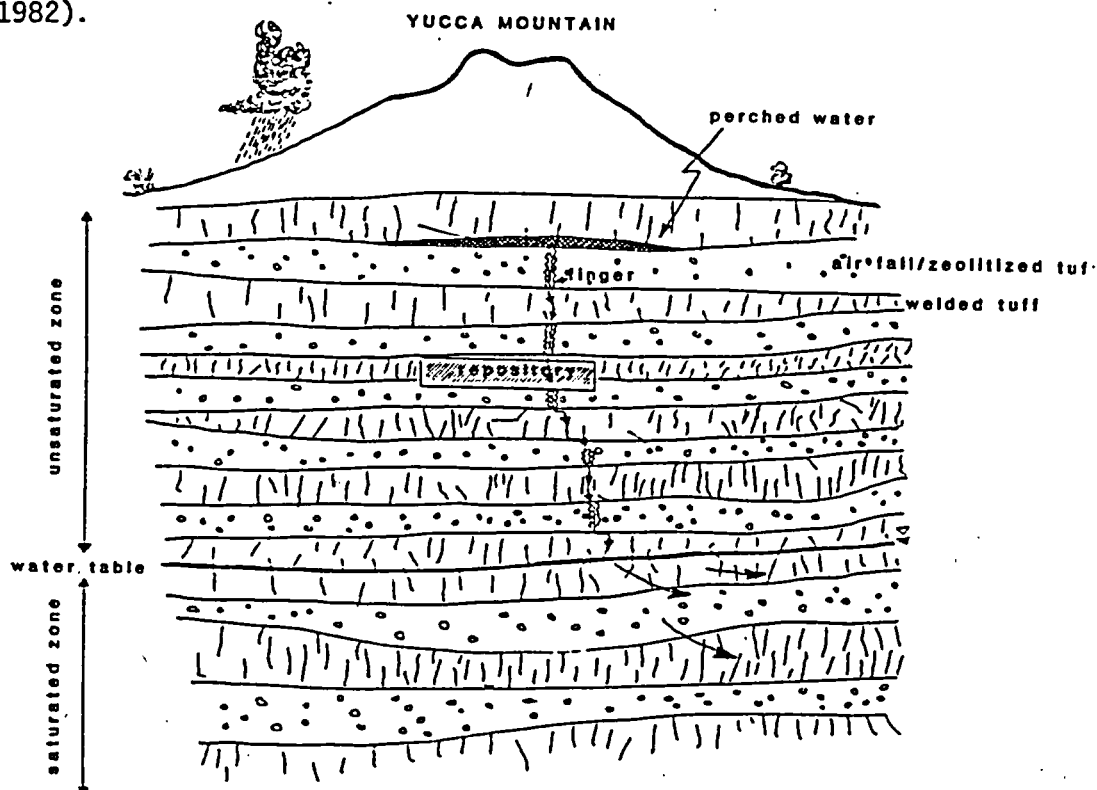


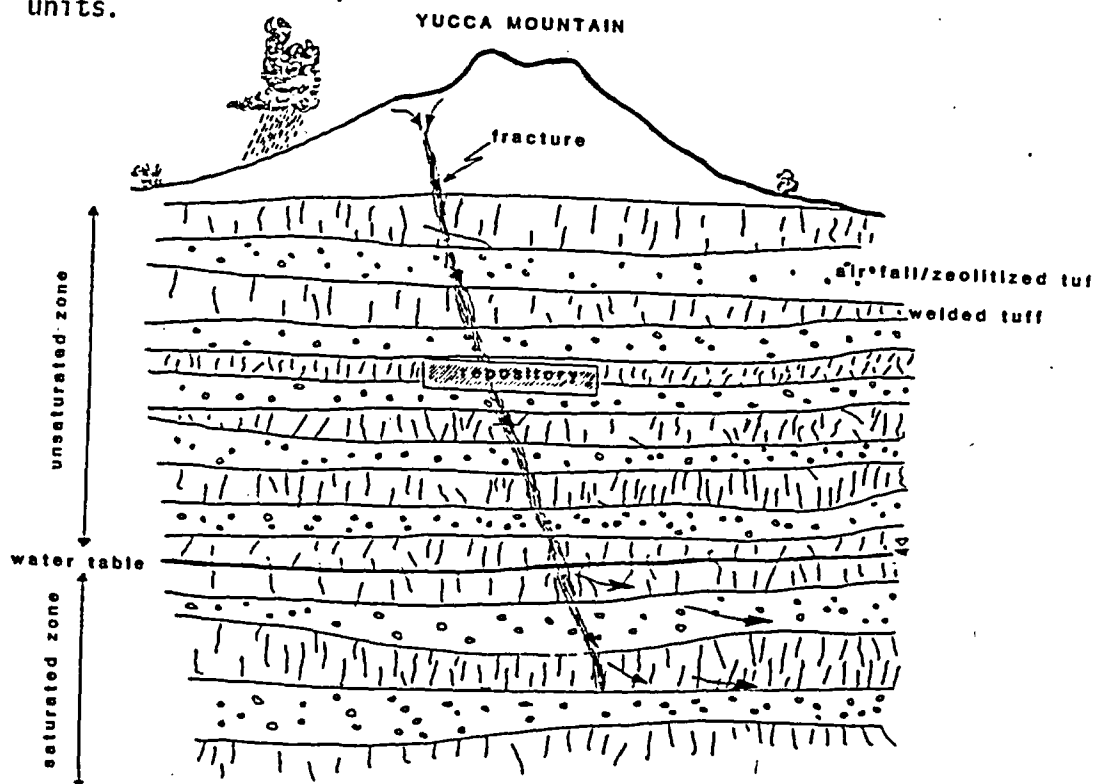
Figure 5. Diagram of NTS Fingering Scenario.

In this scenario, infiltrating water perches in the horizons above and/or below the repository. This water then flushes rapidly through the highly conductive macropore zone down potential. The water from above the repository intercepts the wastes to increase the local water content around the canisters. Wastes that leach into the water are then transported to the phreatic zone either by continued fingering through the porous units (repetitive fingering) or through normal infiltration without perching and fingering. Water might also perch above the Calico Hills Tuff below the repository horizon. Water that has already contacted the wastes and is transporting the contaminants downward may pond above and within this unit. Fingering could transport the radionuclides much more rapidly to the phreatic zone than a calculation based on the assumption of darcy flow might predict. Rapid transport would effectively shorten travel times of the radionuclides, but the additional time for saturation to occur prior to fingering might compensate for the shortened transit times. Perhaps the travel times calculated with darcy flow will be equal to those of this scenario with fingering in a transient flow field. As fracture flow will dominate in the welded tuffs, fingering can only occur as pulses through the more porous air fall and zeolitized tuffs, so the importance of fingering may be assessed by estimating the percentage of these units along the transport path to the saturated zone.

#### SCENARIO III: FRACTURE FLOW

Unlike the pulse or flush of water that occurs with fingering, fracture flow may be characterized as relatively constant seepage if the fractures are interconnected and recharged at a fairly constant rate. Fractures within this scenario include continuous structural discontinuities with

hydraulic conductivities at least one order of magnitude greater than the conductivities of the host rocks. As these structures are best maintained in the more competent strata, they may or may not transect the air fall and zeolitized tuff units. Discrete fracture sets unique to a flow unit are not considered because they provide the principal hydraulic conductivity of the unit and probably will not continue into the units above and below. Faults, flexure zones, fracture trace structures, and lineaments are considered since they more likely transect several flow units.



### NTS RELEASE SCENARIO

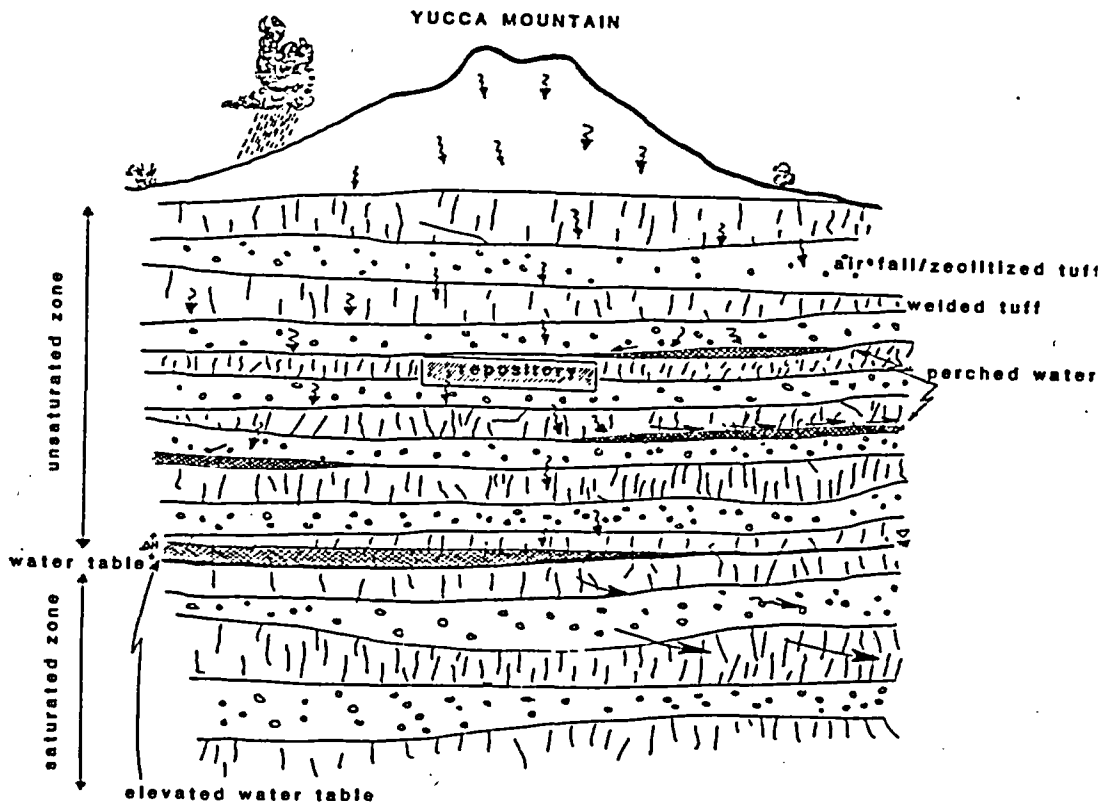
Figure 6. Diagram of NTS Fracture Flow Scenario.

If such a feature was discovered during the construction of a HLW repository, it might be assumed that standard engineering techniques (e.g. grouting, shaft sealing, etc.) might substantially reduce the hydraulic conductivity of the fracture, thereby eliminating this scenario from consideration. However, since the fracture could provide a rapid hydraulic connection with the saturated zone beneath the repository and transport radionuclides to the accessible environment faster than predicted if darcy flow occurs in the flow units, the fracture scenario cannot be eliminated from consideration. In this scenario, recharge from the surface above the repository site funnels into the fracture, intercepts the repository, and flows down to the water table. Once in the saturated zone, the contaminated groundwater flow in response to the regional hydraulic gradients. The fracture is assumed to be continuous across the various flow units and conducts water through the unsaturated zone to the saturated zone. Despite the high negative potentials in the tuff matrix within the unsaturated zone, it is assumed that no water is lost to the matrix as the recharge infiltrates along the fracture. Within the saturated zone, the same fracture provides a zone of increased hydraulic conductivity compared to the conductivity of the saturated units.

#### SCENARIO IV: PERCHED AND ELEVATED TABLES

Perched water may already be present within the Tertiary tuffs at Yucca Mountain given the low hydraulic conductivities and porosities of many of these units. During pluviation, surface infiltration may increase in response to increased precipitation. As infiltration increases, already perched lenses may enlarge, new portions of the vadose zone may saturate, and the regional water table may rise. The pluviation that occurred

throughout portions of the Basin and Range Physiographic Province during the late Wisconsinan Glacial Stage formed stagnant lakes within the intermontane valleys. Although recent studies of NTS and the Yucca Mountain site indicate that infiltration did not increase significantly during this pluvial period, changes in weather patterns and climate could alter the arid environment at Yucca Mountain and increase infiltration into the vadose zone.



**NTS RELEASE SCENARIO**

Figure 7. Diagram of NTS Perched and Elevated Tables Scenario.

As infiltration increases, the capacity of the unsaturated flow system to conduct all percolating waters to the phreatic zone and maintain steady state flow may be exceeded, thereby saturating portions of the unsaturated zone above the regional water table. Water may perch within and above the less conductive flow units. If perched lenses enlarge, horizontal hydraulic gradients within the perched lenses may induce lateral flow downdip from the repository. If the perched water has already contacted the waste and leached radionuclides, the contaminants could be transported an appreciable lateral distance prior to reaching the saturated zone. If water perches above the repository, fingering could again flood the repository with water and transport the radionuclides to the water table. The perched lenses could provide alternate transport paths for radionuclides from the repository.

Another response of the system to prolonged increased recharge might be the elevation of the regional water table. Although the high transmissivities of the welded tuffs might prevent any rise in the water table by rapidly conducting the excess water down gradient, any dramatic rise in the water table must be evaluated as it may provide a shortened transport path through the unsaturated zone. As the water table rises, the hydraulic gradient would also increase resulting in decreased travel times through the unsaturated zone. Both the rise in the regional water table and the establishment of perched lenses within the variably saturated zone could provide pathways along which groundwater travel times would be significantly reduced and, therefore, the perched tables scenario must be analyzed.

## SCENARIO V: HYDROTHERMAL VENTING AND GAS/VAPOR PHASE FLOW

Accounting for dramatic thermal effects in repository performance, this scenario details potential hydrothermal venting of vadose zone waters that are conducted into a hot repository along open fractures. Once the cool waters reach the hot repository, they flash into steam and escape through transmissive fractures to the surface. The steam transports contaminated water (with leached radionuclides) and gaseous fission products, which escape directly to the accessible environment. Although this scenario details a potential release pathway for radionuclides from the repository, it may be considered unlikely. The hydrothermal scenario highlights, however, the potential for vapor and gas phase transport of radionuclides through the unsaturated zone. The atmosphere and land surface are the closest accessible environments to the repository. phase transport through the unsaturated zone.

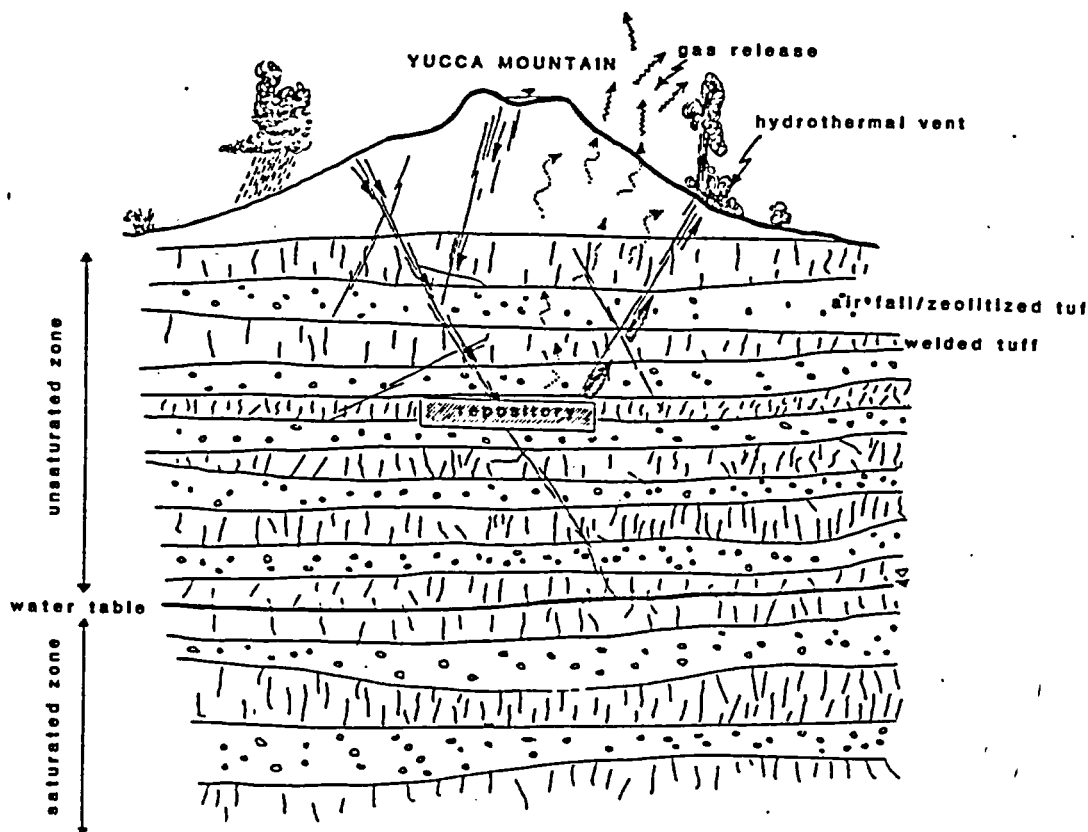
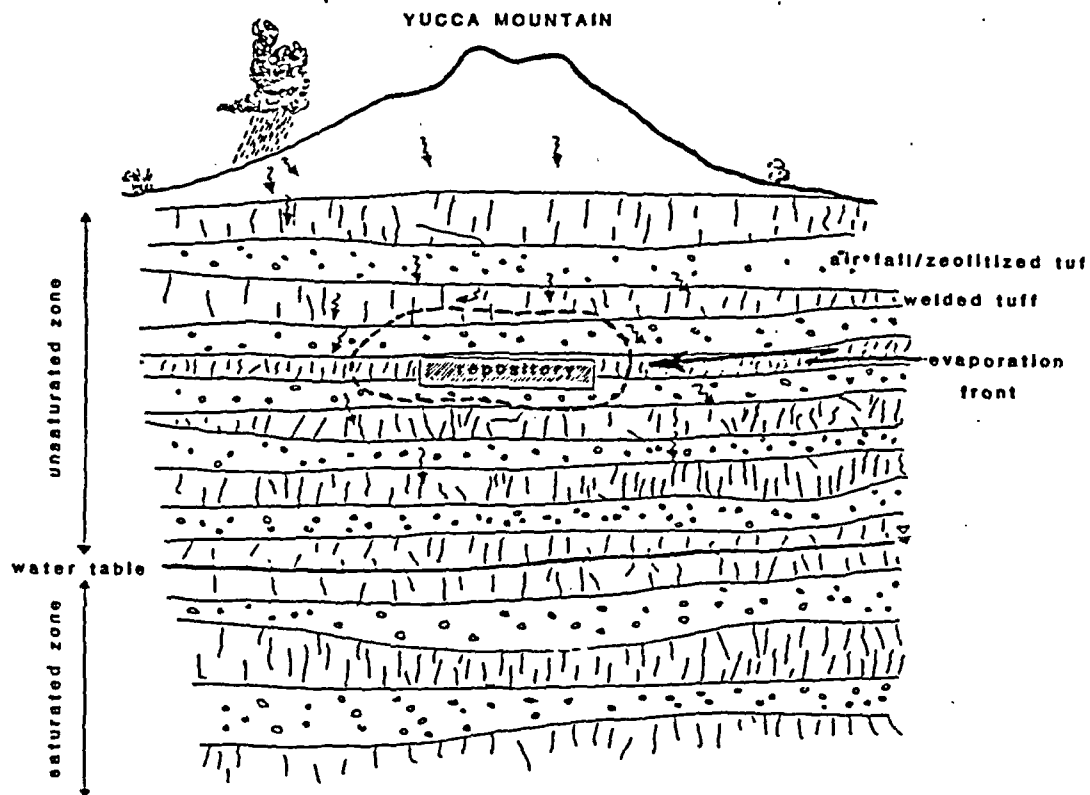


Figure 8. Diagram of NTS Hydrothermal Venting Scenario.

Gaseous fission products like Kr85, Xe126, and C14 (in CO<sub>2</sub>) will be generated during fuel cycle decay and released to the surface. Since these discharges could violate the EPA release limits, this scenario should address not only the effects of steam venting, but also vapor and gas

#### SCENARIO VI: DRY REPOSITORY

If the temperature of the repository increases above the boiling point of water (approximately 100 °C) and the hydraulic conductivity of the host rock is sufficiently low to prevent rapid flushes of percolating water, the repository may remain dry during the early history of the site. As the temperature increases above the ambient temperature, evaporation of water within the host rock will increase. The produced vapor will migrate away from the highest temperature areas and condense at some distance from the repository as it is driven by the pressure gradient. Pore pressure will be highest in the repository as the air within the pores expands. As the temperature continues to increase, all liquid water within the repository will be vaporized. A vaporization front will propagate away from the repository. A condensation front will also form at some distance from the repository where the ambient temperature is less than 100 °C. Moisture will, therefore, migrate from the vaporization front to the wetting or condensation front. Nominal volumes of water may be drawn back into the repository to replenish the water that has been vaporized. Most of the water, however, would be forced away from the repository by pressure and thermal gradients so that the repository would remain dry as long as enough heat is produced. This process prevents water from entering the containment area and reacting with or leaching the wastes. The repository becomes essentially isolated from the subsurface water flow system, thus fulfilling the objective of a HLW repository.



### NTS RELEASE SCENARIO

Figure 9. Diagram of NTS Dry Repository Scenario.

Once most of the heat energy has escaped from the repository, the repository will begin to cool, the vapor and condensation fronts will recede, and infiltrating water may once again contact the wastes. The time delay during the isolation of the repository may be sufficient to comply with the release limits of the EPA and NRC during the first 10,000 years. This thermal effect provides a time buffer for the repository in the unsaturated zone. This subject has been further developed in the heat flow estimate calculations included in this paper (refer to Appendix A).

MODELING METHODOLOGY

A modeling methodology designed to evaluate repository performance for the above mentioned scenerios has been developed. However, it is still in an early stage of development since many of the hydrologic and thermal processes described in these scenerios cannot be simulated by the computer codes used. This modeling methodology will evolve as the NRC's computer modeling capabilites grow.

The modeling methodology can best be described by way of demonstration. What follows is an illustrative modeling excercise of the unsaturated zone designed to illustrate: 1) the types of data required in modeling the unsaturated zone, 2) the assumptions made, 3) the problems encountered, 4) the output produced, and 5) how the flow model may be coupled to a transport model. Ultimately, flow and transport models for both the saturated and unsaturated zones will be coupled in such a way so as to describe radionuclide flow paths in a continuous manner from the repository to a far-field/discharge location.

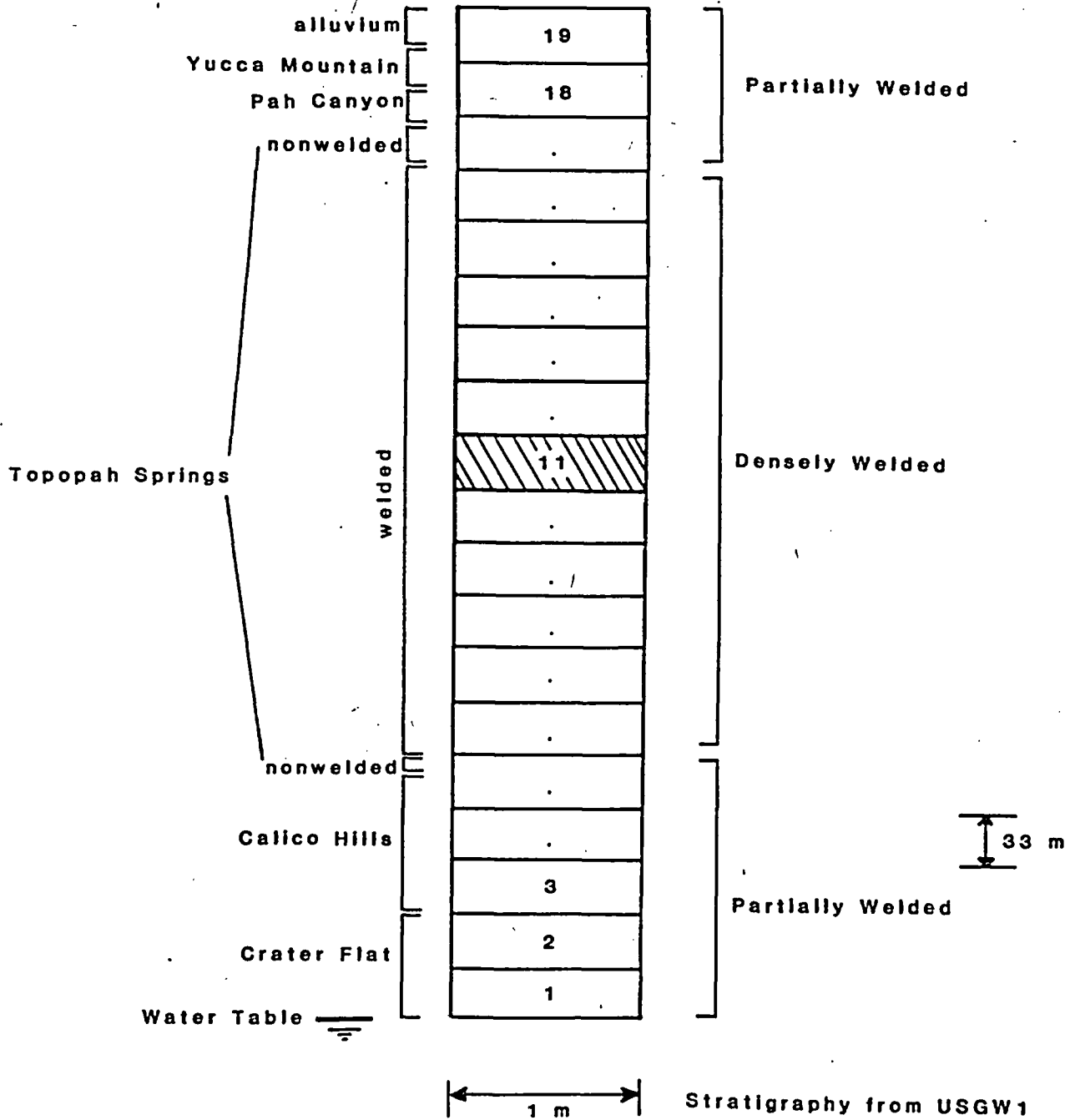
Unsaturated Flow

The FEMWATER code is used in this study because of its ease of implementation. It is a finite element code that simulates two dimensional isothermal flow through variably saturated media. It allows for several different materials or media, requiring soil moisture characteristic curves as input for each one.

FEMWATER is used to simulate one-dimensional, steady-state, isothermal flow through a column representing a simplified stratigraphy of the unsaturated zone beneath Yucca Mountain. The model grid (Figure 10) extends from the land surface down to the water table and consists of 19 elements, each measuring 33 M x 1 M. The boundary conditions consist of no-flow boundaries on the sides, a zero pressure (atmospheric) boundary on the bottom representing the water table, and a constant flux (3 mm/y) boundary on the top representing surface infiltration. The stratigraphy has been simplified into three tuff units: the upper and lower units are partially welded, and the middle unit is densely welded. The densely welded tuff was assigned a lower porosity and a higher conductivity than the partially welded tuff. The lower porosity is due to its denser composition, and the higher conductivity is due to its higher fracture frequency. The values used for the porosity and saturated conductivity are:

	Porosity (cm <sup>3</sup> /cm <sup>3</sup> )	Conductivity (cm/s)
Densely Welded	15	1.0E-4
Partially Welded	30	1.0E-6

3mm/yr



### FINITE ELEMENT GRID OF YUCCA MOUNTAIN UNSATURATED ZONE

Figure 10. Finite element grid of the unsaturated zone below Yucca Mountain executed with FEMWATER.

These data were derived from data made available by the USGS prior to the NTS workshop (January, 1983).

The variably saturated hydraulic conductivities required as input into FEMWATER were obtained from soil-moisture characteristic curves. Since these curves are not currently available for the Yucca Mountain tuffs, the curves were derived from the FEMWATER user's manual (NUREG/CR-2705).

Results of this exercise (refer to Appendix A for a listing of the input and output) show vertical seepage velocities to be very small throughout the column. Groundwater travel time from a repository located in the center of grid element 10 (approximately 1000 feet above the water table) is nearly 25,000 years.

Since permeability values greater than strictly matrix permeability were incorporated into the hydraulic conductivity terms, the effects of discrete fracture flow has been slightly mitigated. Codes that allow for matrix and fracture flow in the unsaturated zone are being developed. However, even if such codes were readily available, characterization of the unsaturated fracture flow input parameters will not be readily determinable.

In summary, this portion of the modeling methodology proved to be easy to implement, but suffered from weaknesses such as data insufficiencies (generic to all unsaturated flow modeling), and the assumption of strictly porous flow under isothermal conditions. However, FEMWATER is a very versatile code and should be useful in evaluating unsaturated flow data and interpretations that might be presented by DOE in support of site characterization.

Radionuclide Transport Model

Using the computed water flow velocities and pressure heads of the one-dimensional FEMWATER model, radionuclide transport may be modeled from the repository to the accessible environment with the generalized version of NWFT/DVM. While FEMWASTE, a finite element transport code for modeling variably saturated media, was written to couple with FEMWATER, applications of FEMWASTE to assessing repository performance are limited because it can only model one radionuclide or contaminant per execution run. During the lifetime of a HLW repository, it is expected that several radionuclides will be released, and as the isotopes with shorter half-lives decrease in total concentration, longer-lasting isotopes will dominate the released inventory. Generalized NWFT/DVM, written by Cranwell and Shortencarrier at SNL, computes decay, release, adsorption, and transport of up to 120 radionuclides in as many as six branching decay chains.

Prior to a discussion of the assumptions and results of the radionuclide transport model using generalized NWFT/DVM, it should be stressed that the results of this modeling exercise do not reflect preliminary approval of the Yucca Mountain site as a HLW repository. Even though the minimum groundwater travel times exceed 40,000 years, rigorous performance assessment of groundwater flow and transport at NTS is premature. The physics and mechanics of flow within the unsaturated zone are themselves poorly understood, and because numerical models approximate the equations that describe these physical processes, groundwater flow and transport models through variably saturated media are only in their developmental stages. If contemporary computer codes could simulate unsaturated hydrodynamics concurred upon by hydrologists studying vadose

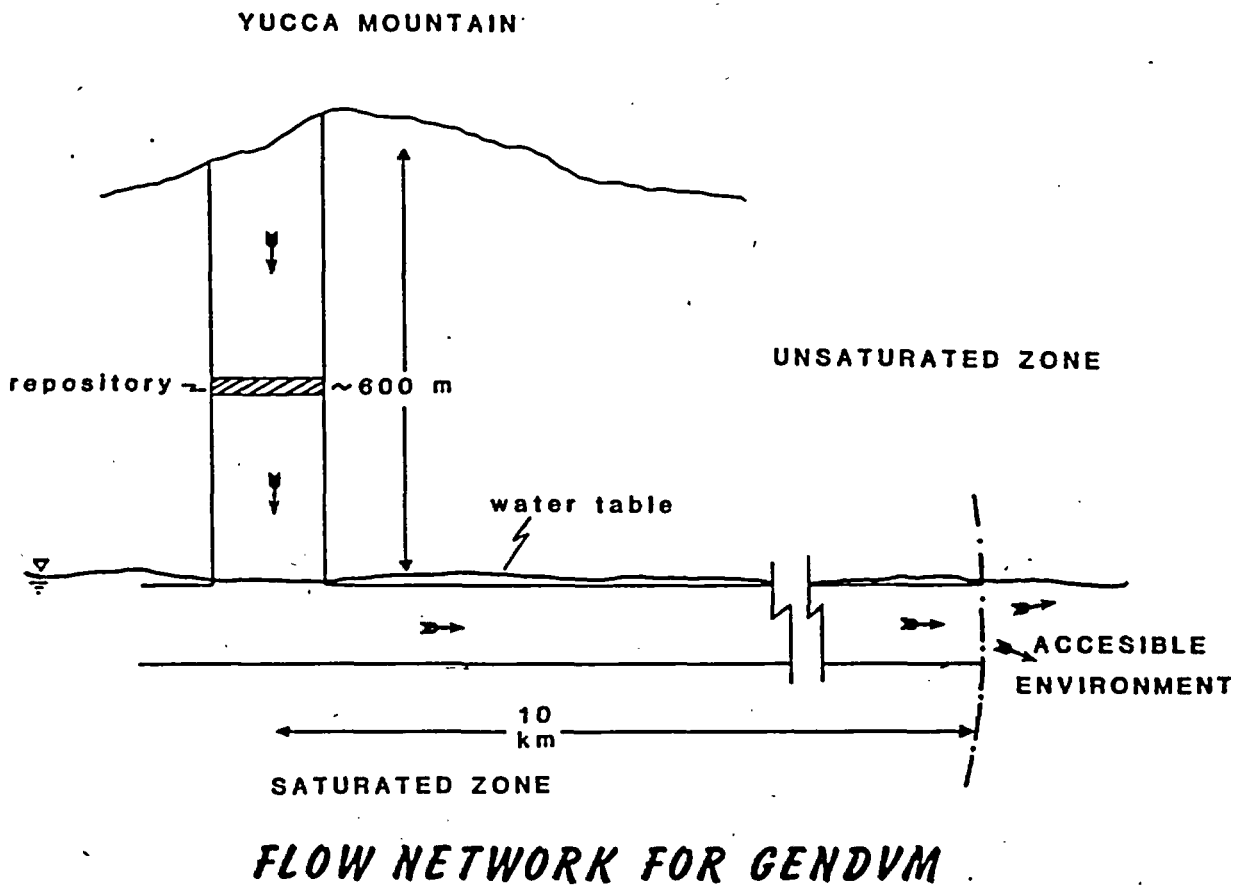


Figure 11. Generalized flow network for the coupled unsaturated-saturated flow system executed with GENDVM.

zone flow, the paucity of available data would prevent their predictive application to repository performance assessment. In addition to the uncertainties in the hydrologic system, uncertainties of equivalent, if not greater, magnitude occur in the geochemical characterization of the vadose zone. Questions about the existence of chemical and thermal equilibrium, permanent or transient sorption, precipitation, oxidation, chelation, and vapor phase transport cloud the conceptual model of radionuclide transport through the unsaturated zone at NTS. A clear conceptual model must be formulated prior to the successful application of a numerical model to predict discharges of radionuclides to the accessible environment and assess the performance of a proposed HLW repository. The models detailed in this paper should only be used to provide a general estimate of the minimum groundwater travel time and radionuclide transport along one specified flow path.

The minimum range of uncertainty in the computed travel times alone is six orders of magnitude. A listing of the uncertainties within this transport model are highlighted in the following discussion of the assumptions executed. Generalized NWFT/DVM (GENDVM) is a pipe flow, quasi-three-dimensional, radionuclide transport code. Unlike its predecessors NWFT and NWFT/DVM, GENDVM models a flow system which is entirely specified by the user. In the coupled unsaturated/saturated flow and transport model, the flow system is comprised of 7 legs and 8 junctions. Legs 1 through 5 simulate darcy flow through the unsaturated zone, leg 3 is the repository within the densely-welded Topopah Springs Member, and legs 6 and 7 model darcy flow within the saturated regional flow system. The GENDVM flow network is illustrated in Figure 11.

Although GENDVM is written for flow and transport in saturated media, this model has been adapted to unsaturated media by using the pressure

heads and flow velocities obtained from FEMWATER. The effective hydraulic conductivity of the unsaturated legs is varied to reproduce the total head distribution, flow rates, and velocities through the approximately 600 meters of unsaturated tuffs at Yucca Mountain. The derivation of this conductivity may be most easily illustrated in a listing of the founding assumptions.

- ° Percolation of water through the unsaturated zone is steady state so that the volume flux through the system is zero ( $R_{in} = R_{out}$ ).
- ° The cross-sectional areas of the repository and the pipes is 1 km<sup>2</sup> or 1E6 m<sup>2</sup>.
- ° The volume of flow entering and leaving the unsaturated zone is equal to the annual average infiltration rate ( 3 mm) multiplied by the cross-sectional area of the pipes, or
 
$$Q = R \times A = .003\text{m/yr} \times 1\text{E6 m}^2, \text{ and}$$

$$Q = 3\text{E3 m}^3/\text{yr}.$$
- ° The total head gradient is constant through the unsaturated zone and equal to 0.198 as calculated using FEMWATER output.
- ° Water velocity is constant through the unsaturated zone and equal to 9.5E-9 cm/s as calculated in FEMWATER.
- ° The equivalent hydraulic conductivity is constant within the unsaturated zone and equal to 4.79E-10 m/s (1.36E-4 ft/d), or

$$Q = KIA, \text{ so}$$

$$u = Q/A = KI,$$

$$u/I = K, \text{ and}$$

$$u/I = 9.5\text{E-9}/.198 = 4.79\text{E-8 cm/s (1.36E-4 ft/d)}.$$

Water that leaves the unsaturated zone enters the regional saturated flow system represented by legs 6 and 7. The prescribed hydraulic gradient across this flow path within the phreatic zone is 3.0E-2, a gradient typical of the lower conductivity units at NTS (see the Tuff RSD).

Pertinent geochemical data for this model are listed in Tables I and II. The values for the solubilities of the major radionuclides considered (C14, Ni59, Sr90, Tc99, U234, and Pu239) were derived from data presented in the Tuff Site RSD. Similarly, the  $R_d$  values used in this model were converted from the retardation coefficients listed in the RSD. It is important to reiterate the limitations of this radionuclide transport model. Realistic values for distribution coefficients of radionuclides within the unsaturated zone are currently unknown. Upper bounds are difficult to develop and support. While the lowest value would be zero with no retardation, the highest  $K_d$  values may exceed those of the saturated zone if permanent sorption and precipitation readily occur in the unsaturated zone.

Initial inventories of radionuclides in the repository were computed using the computer code ORIGEN for a 100,000 MTHM repository. The radionuclides chosen for this model were selected based upon sensitivity analyses prepared by NRC, SNL, and Golder Associates. The leach time is specified as 100,000 years, so that the release of radionuclides whose solubility limits exceed one part in one hundred thousand will be released according to leach limitation. Waste leaching begins at 1000 years. The flow properties of the legs and their retardation coefficients are listed in Tables III and IV.

### Results

Groundwater travel times calculated by GENDVM agree with those calculated with FEMWATER of approximately 25,000 years through the unsaturated zone below Yucca Mountain. Total travel times from the repository to the accessible environment exceed 40,000 years. A survey of the output from

TABLE I. RADIONUCLIDE SOLUBILITIES

<u>Radionuclide</u>	<u>Solubility<sup>*</sup></u> <u>(in molality)</u>
C14	-----
Ni59	-----
Sr90	10E-3.3
Tc99	-----
U234	10E-4.6
Pu239	10E-15.9

\* assuming a dilute aqueous solution with pH=7.00 and Eh=+0.45 V

(Siegel, M.D. (1982) "Geochemistry," in Tuff Repository Site Definition, Sandia National Laboratory, p. 31).

TABLE II. RETARDATION COEFFICIENTS OF RADIONUCLIDES

<u>Radionuclide</u>	<u>Rd (ml/g)<sup>®</sup></u>
C14	0.0
Ni59	0.0
Sr90	300.0
Tc99	0.8
U234	7.0
Pu239	1000.0

® As determined with laboratory analyses of saturated tuffs. May represent disequilibrium values.

(Siegel, M.D. (1982) "Geochemistry," in Tuff Repository Site

Definition, Sandia National Laboratory).

GENDVM included as Appendix C indicates that only C14, Ni59, and Tc99 are discharged to the accessible environment. The carbon and nickel are most easily released from the repository as they are leach-limited radionuclides and are transported without wall-rock retardation in the saturated and unsaturated flow systems. Given the solubility limits and retardation coefficients of this model, U234, Sr90, and Pu239 are significantly retarded in the flow systems and do not escape to the accessible environment ten kilometers distant from the repository.

#### THERMAL CONDITIONS

Within the first several hundred years after emplacement of the proposed repository, significant amounts of heat will be generated by the decay processes of the radioactive waste. This heat is expected to impact the surrounding hydrological and geological environment. The thermal effects will cause the rocks adjacent to the repository to expand, thereby closing up some of the existing fractures within them and effectively lowering their hydraulic conductivities. Other thermal effects include altering the density of contiguous groundwater (thereby inducing a bouyancy gradient) and increased evaporation of the groundwater.

The thermal aspects of repository emplacement in the unsaturated zone are complex and an in-depth discussion is beyond the scope of this paper. The NRC presently does not have a computer code capable of simulating nonisothermal conditions in the unsaturated zone; however several codes exist which might be applicable and are being scrutinized for possible inclusion into the NRC program. It should be noted that the state of the technology is such that there exists no code which fully accounts for all

Table III. Hydraulic Flow Characteristics of Legs within the GENDVM Network.

		LEG PROPERTIES						LEG PROPERTIES			
LEG 1		LENGTH =	3.25E+02 FT		LEG 4		LENGTH =	5.41E+02 FT			
*****		AREA =	1.08E+07 FT**2		*****		AREA =	1.08E+07 FT**2			
		CONDUCTIVITY =	4.96E-02 FT/YR				CONDUCTIVITY =	4.96E-02 FT/YR			
		POROSITY =	.3000				POROSITY =	.1500			
		ROCK DENSITY =	1.19E+02 LB/FT**3				ROCK DENSITY =	1.45E+02 LB/FT**3			
		FLUID DENSITY =	6.23E+01 LB/FT**3				FLUID DENSITY =	6.23E+01 LB/FT**3			
		BRINE CONCENTRATION =	0.				BRINE CONCENTRATION =	0.			
		LEG PROPERTIES						LEG PROPERTIES			
LEG 2		LENGTH =	5.41E+02 FT		LEG 5		LENGTH =	5.41E+02 FT			
*****		AREA =	1.08E+07 FT**2		*****		AREA =	1.08E+07 FT**2			
		CONDUCTIVITY =	4.96E-02 FT/YR				CONDUCTIVITY =	4.96E-02 FT/YR			
		POROSITY =	.1500				POROSITY =	.3000			
		ROCK DENSITY =	1.45E+02 LB/FT**3				ROCK DENSITY =	1.19E+02 LB/FT**3			
		FLUID DENSITY =	6.23E+01 LB/FT**3				FLUID DENSITY =	6.23E+01 LB/FT**3			
		BRINE CONCENTRATION =	0.				BRINE CONCENTRATION =	0.			
		LEG PROPERTIES						LEG PROPERTIES			
LEG 3		LENGTH =	1.08E+02 FT		LEG 6		LENGTH =	3.28E+02 FT			
*****		AREA =	1.08E+07 FT**2		*****		AREA =	1.08E+07 FT**2			
		CONDUCTIVITY =	4.96E-02 FT/YR				CONDUCTIVITY =	3.10E+00 FT/YR			
		POROSITY =	.0100				POROSITY =	.0500			
		ROCK DENSITY =	1.68E+02 LB/FT**3				ROCK DENSITY =	1.62E+02 LB/FT**3			
		FLUID DENSITY =	6.23E+01 LB/FT**3				FLUID DENSITY =	6.23E+01 LB/FT**3			
		BRINE CONCENTRATION =	0.				BRINE CONCENTRATION =	0.			
		LEG 7						LEG 7			
		LENGTH =	3.17E+04 FT				LENGTH =	3.17E+04 FT			
		AREA =	1.08E+07 FT**2				AREA =	1.08E+07 FT**2			
		CONDUCTIVITY =	3.10E+00 FT/YR				CONDUCTIVITY =	3.10E+00 FT/YR			
		POROSITY =	.0500				POROSITY =	.0500			
		ROCK DENSITY =	1.62E+02 LB/FT**3				ROCK DENSITY =	1.62E+02 LB/FT**3			
		FLUID DENSITY =	6.23E+01 LB/FT**3				FLUID DENSITY =	6.23E+01 LB/FT**3			
		BRINE CONCENTRATION =	0.				BRINE CONCENTRATION =	0.			

Table IV. Assumed Distribution Coefficients and Retardation Factors for the Transported Radionuclides used in the GENDVM model.

DISTRIBUTION COEFFICIENTS(KD) AND RETARDATION FACTORS(R) FOR CHAIN 1							
LEG		C14	N159	SR90	TC99	U234	PU239
1	3	KD 0.	0.	4.810E+00	1.280E-02	1.120E-01	1.603E+01
		R 1.000E+00	1.000E+00	8.095E+04	2.164E+02	1.886E+03	2.698E+05
2	4	KD 0.	0.	4.810E+00	1.280E-02	1.120E-01	1.603E+01
		R 1.000E+00	1.000E+00	4.635E+03	1.333E+01	1.089E+02	1.544E+04
3	5	KD 0.	0.	4.810E+00	1.280E-02	1.120E-01	1.603E+01
		R 1.000E+00	1.000E+00	1.909E+03	6.077E+00	4.543E+01	6.360E+03
4	7	KD 0.	0.	4.810E+00	1.280E-02	1.120E-01	1.603E+01
		R 1.000E+00	1.000E+00	1.554E+04	4.234E+01	3.628E+02	5.178E+04

the significant processes that might be present in an unsaturated nonisothermal system.

If gross simplifications can be assumed, the effects attributed to several of these processes might be calculated from simplified "back of the envelope" equations. Examples are given in Appendix A in which calculations of some of the thermally induced phenomena are presented.

### CONCLUSIONS

In summary, a methodology has been presented which outlines how various NRC performance codes may be linked together to evaluate repository performance, and with which NRC may perform sensitivity studies of the hydrological and geochemical parameters governing the transport of radionuclides through the unsaturated zone.

On a larger scale, the methodology presented is a small but integral portion of the overall NRC performance assessment scheme. In order to describe the flow path of a radionuclide from a repository to the accessible environment, the regional flow regime must be conceptually understood. The conceptualization would then be translated into input for a computer code (e.g., SWIFT) which would be used to define the saturated flow conditions around Yucca Mountain. A higher resolution gridding of the Yucca Mountain area is then needed to define the saturated flow conditions beneath Yucca Mountain. At this juncture, the methodology presented would be used to determine a radionuclide flow path from the repository down to the zone of saturation. A far-field

transport code (e.g., SWIFT or GENDVM) may then be used to track the radionuclide(s) to the accessible environment.

The conclusions of this modeling program provide a framework for subsequent performance assessments of the proposed repository at Yucca Mountain. The results generated by FEMWATER and GENDVM are valid for the following assumptions:

- that porous media flow calculations are valid in estimating groundwater flow through both the unsaturated and saturated flow systems;
- that single differential heads can be properly specified to exist across entire flow paths (i.e. through the unsaturated/saturated zones);
- that flow can be effectively modeled for this flow system by using a quasi-two-dimensional, isothermal, steady-state, network radionuclide transport model;
- that the equivalent hydraulic conductivities assigned in the GENDVM model effectively simulate vadose zone flow velocities and recreate the total head distribution within the unsaturated zone;
- that the solubilities, retardation coefficients, and initial inventories are representative of the physical repository environment;
- that the unsaturated flow system exists in a steady state so that the 3 mm of annual infiltration does not exceed the capacity of the system to conduct the supplied recharge; and

° that the thermal effects of the repository are nominal and water flows through the unsaturated zone purely in response to gravity.

It can be argued that these assumptions oversimplify the variably-saturated-and saturated flow systems at NTS. This modeling program, however, was not designed to provide deterministic travel times and radionuclide discharges to the accessible environment. With the void of knowledge about groundwater flow and radionuclide transport in the unsaturated zone, the authors of this paper emphasize the need for more detailed site characterization and research into variably saturated systems prior to realistic assessment of a repository at Yucca Mountain. The results of the FEMWATER and GENDVM models were not included in this report to demonstrate compliance of a hypothetical repository to release standards proposed by EPA, but rather to provide rough estimates of groundwater travel times and discharges of radionuclides to the environment along the assumed flow path, thus coupling the saturated and unsaturated flow systems at NTS. This modeling program demonstrates the NRC's capability of assessing the performance of a proposed HLW repository at Yucca Mountain.

## APPENDIX A

### Heat Induced Groundwater Vacancy

If the repository temperature exceeds 100°C, water present in the contiguous rock matrix and fractures will be evaporated. Shortly thereafter, a 100°C isotherm will exist at some distance from the repository within which all water will have been evaporated (refer to Figure \_\_\_\_). The presence and extent of this dried out zone is

significant in many ways: 1) it may serve as a buffer from groundwater infiltration resulting in a completely dry repository, 2) hydrofracturing might occur during evaporation which would result in an envelope of increased permeability; this may facilitate flow when the temperatures recede below 100°C, and 3) a zone of increased saturation could be expected at the <100°C / >100°C interface due to condensation of the evaporated water; this would result in increased permeability at the interface.

The thermal source driving the heat into the rock units is the thermal loading of the HL waste. The heat will be removed by conduction in the rock matrix, and also by groundwater and vapor transport. Perhaps the most significant process in removing the heat will be due to evaporation of groundwater within the rocks surrounding the repository and recondensation of the vapor some distance away. This will be a continuous process since groundwater will continue to infiltrate towards the repository from above. At some point in time, the heat removed through evaporation will exceed the heat produced from the repository and ambient saturation will again be established throughout the host rock.

A simplistic methodology of calculating the volume and extent of the "dry" zone is presented below. Many simplifying assumptions are made and therefore results based on this methodology should be taken as a "ballpark" estimate only. These assumptions are listed below:

The repository may be represented by a point heat source.

A rectangular repository is emplaced in a homogeneous (thermal properties) medium.

Complete evaporation occurs where rock temperature exceeds 100°C.

The evaporation process can be decoupled from other thermally induced processes.

Atmospheric pressure exists from the surface to the water table./

The 100°C isotherm may be represented as a sphere about the repository.

Thermal convection through the rock matrix and groundwater evaporation are the only significant heat removal processes.

Let  $r_1$  be the radial distance from the source to the 100° isotherm.

Let  $r_2$  be the radial distance from the source to where ambient temperatures would be expected.

Let  $T_1 = 100^\circ\text{C}$ ,

$T_2 =$  ambient temperature,

$Q =$  initial heat output in watts,

$K =$  thermal conductivity of the medium.

The heat flow from a point source in a sphere is defined as:

$dT$

$$Q = -K48r^2 \frac{dr}{dr}$$

Solving for  $r_1$  yields:

$$r_1 = \frac{r_2}{1 + r_2 \left( \frac{48K}{Q} (T_1 - T_2) \right)}$$

$r_1$  now gives us the approximate extent of the 100° isotherm (Figure ).

The amount of infiltration that will intercept the 100°C isotherm is:

$$\text{Amt. inf} = (\text{inf. rate})(8r_1^2)$$

The heat consumed would be:

Heat Consumed = (Amt. inf.)(Latent Heat Vaporization)

The removal of heat due to evaporation would effectively reduce  $r_1$ . When the heat produced by the repository (Q) is less than the heat consumed (due to evaporation of infiltration directly over the repository), the "dry" zone will cease to exist and ambient saturation will return to ambient conditions.

#### REFERENCES

Campbell, J.E., Longsine, D.E., and Cranwell, R.M., Risk Methodology for Disposal of Radioactive Waste: The NWFT/DVM Computer Code Users Manual, NUREG/CR-2081, 1981.

Ehlers, E.G., and Blatt, H. Petrology: Igneous, Sedimentary, and Metamorphic, (San Francisco: W.H. Freeman and Company, 1982).

Freeze, R.A., and Cherry, J.A. Groundwater, (Englewood Cliffs, New Jersey: Prentice-Hall, Inc., 1979).

Lajorie, J., "Volcaniclastic Rocks," in Walker, E.G. (Ed.), Facies Models, Geological Association of Canada, 1980.

Siegel, M.D., "Geochemistry," in Tuff Repository Site Definition (Draft), Sandia National Laboratory, 1982.

Simpson, T.W., and Cunningham, R.C., "The occurrence of Flow Channels in Soils," Journal of Environmental Quality, v. 11, no. 1, 1982,

pp. 29-30.

Sinnock, S., Geology of the Nevada Test Site and Nearby Areas, Southern Nevada, Sandia National Laboratory, SAND82-2207, 1982.

Yeh, G.T., Training Course No. 1: The Implementation of FEMWATER Computer Program, NUREG/CR-2705, 1982.

1	NTS	UNSAT	1-D	1/A3								10		
40	19	2	0	0	0	1	15	1	0	1	0	30	10	5
1	1													
	100.		1.0		100.0		100.0		0.0		1.0E-3		0.0	1.0
	981.		1.0		0.5									

5  
11

	0.0		0.0		0.30		1.0E-6		1.0E-6					
	0.0		0.0		0.15		1.0E-4		1.0E-4					
	-400.		-200.		-175.		-150.		-125.		-100.0		-62.5	-50.0
	-37.5		-25.		-12.5		0.		50.		100.		2000.	
	-400.		-200.		-175.		-150.		-125.		-100.0		-62.5	-50.0
	-37.5		-25.		-12.5		0.		50.		100.		2000.	
	.0032		0.00425		0.0045		0.005		0.00625		0.009		0.021	0.025
	.0275		0.0285		0.029		0.0295		0.02975		0.02995		0.03	
	.0032		0.00425		0.0045		0.005		0.00625		.009		0.021	0.025
	.0275		0.0285		0.029		0.0295		0.02975		0.02995		0.03	
	0.018		0.103		0.190		0.280		0.420		0.5		0.98	1.00
	1.01		1.01		1.01		1.01		1.01		1.01		1.01	
	0.018		0.103		0.190		0.280		0.420		0.5		0.98	1.00
	1.01		1.01		1.01		1.01		1.01		1.01		1.01	
	0.52E-4		0.10E-3		0.20E-3		0.50E-3		0.11E-2		0.32E-2		0.32E-2	.20E-2
	0.80E-3		0.40E-3		0.20E-3		0.10E-3		0.40E-4		0.28E-6		0.0	
	.52E-4		.10E-3		.20E-3		.50E-3		.11E-2		.32E-2		.32E-2	.20E-2
	.80E-3		.40E-3		.20E-3		.10E-3		.40E-4		.28E-6		0.0	

1	0.0		0.0											
2	1.E02		0.0											
3	0.0		33.E02											
4	1.E02		33.E02											
5	0.0		66.E02											
6	1.E02		66.E02											
7	0.0		99.E02											
8	1.E02		99.E02											
9	0.0		132.E02											
10	1.E02		132.F02											
11	0.0		165.E02											
12	1.E02		165.F02											
13	0.0		198.E02											
14	1.E02		198.E02											
15	0.0		231.E02											
16	1.E02		231.E02											
17	0.0		264.E02											
18	1.E02		264.F02											
19	0.0		297.E02											
20	1.E02		297.E02											
21	0.0		330.E02											
22	1.E02		330.E02											
23	0.0		363.E02											
24	1.E02		363.F02											
25	0.0		396.E02											
26	1.E02		396.E02											
27	0.0		429.E02											
28	1.E02		429.E02											
29	0.0		462.F02											
30	1.E02		462.E02											
31	0.0		495.E02											
32	1.E02		495.F02											
33	0.0		528.E02											
34	1.E02		528.E02											
35	0.0		561.F02											
36	1.E02		561.E02											
37	0.0		594.F02											
38	1.E02		594.E02											
39	0.0		627.E02											
40	1.E02		627.F02											

1	1	2	4	3	1	1	5
6	11	12	14	13	2	1	11
17	33	34	36	35	1	1	3
1			-1000.				
40			-1000.				
2	0	1	2	1	2		
	0.0		100.0				
	9.5E-09		9.5E-09				
39	1				0.0		
40	1				0.0		
19	39	40					
1			0.0				
2			0.0				

99999

OUTPUT TABLE 5.. PRESSURE HEADS AT TIME = 0.

, (DELTA = 1.0000E+02), (BAND WIDTH = 7) IT = 0

STEADY-STATE INITIAL CONDITIONS

NODE I PRESSURE HEAD OF NODES I, I+1, ..., I+7

1	0.	0.	-3.2390E+03	-3.2390E+03	-4.7973E+03	-4.7973E+03	-6.3557E+03	-6.3557E+03
9	-7.9140E+03	-7.9140E+03	-9.4723E+03	-9.4723E+03	-1.2755E+04	-1.2755E+04	-1.6038E+04	-1.6038E+04
17	-1.9320E+04	-1.9320E+04	-2.2603E+04	-2.2603E+04	-2.5885E+04	-2.5885E+04	-2.9168E+04	-2.9168E+04
25	-3.2450E+04	-3.2450E+04	-3.5733E+04	-3.5733E+04	-3.9016E+04	-3.9016E+04	-4.2298E+04	-4.2298E+04
33	-4.5581E+04	-4.5581E+04	-4.7139E+04	-4.7139E+04	-4.8697E+04	-4.8697E+04	-5.0256E+04	-5.0256E+04

OUTPUT TABLE 6.. TOTAL HEADS AT TIME = 0.

,(DELTA = 1.0000E+02),(BAND WIDTH = 7) IT = 0

STEADY-STATE INITIAL CONDITIONS

NODE I TOTAL HEAD OF NODES I,I+1,...,I+7

1	0.	0.	6.0992E+01	6.0992E+01	1.8027E+03	1.8027E+03	3.5443E+03	3.5443E+03
9	5.2860E+03	5.2860E+03	7.0277E+03	7.0277E+03	7.0451E+03	7.0451E+03	7.0625E+03	7.0625E+03
17	7.0799E+03	7.0799E+03	7.0973E+03	7.0973E+03	7.1147E+03	7.1147E+03	7.1322E+03	7.1322E+03
25	7.1496E+03	7.1496E+03	7.1670E+03	7.1670E+03	7.1844E+03	7.1844E+03	7.2018E+03	7.2018E+03
33	7.2192E+03	7.2192E+03	8.9609E+03	8.9609E+03	1.0703E+04	1.0703E+04	1.2444E+04	1.2444E+04

OUTPUT TABLE 8., Darcy Velocities at Time = 0.

(DELTA = 1.0000E+02), (BAND WIDTH = 7) IT = 0

STEADY-STATE INITIAL CONDITIONS

NODE	VX	VZ	NODE	VX	VZ	NODE	VX	VZ	NODE	VX	VZ
1	3.108E-20	-1.621E-08	2	3.197E-20	-1.621E-08	3	1.328E-20	-5.245E-09	4	1.377E-20	-5.245E-09
5	8.149E-21	-1.064E-08	6	6.795E-21	-1.064E-08	7	-1.718E-21	-9.195E-09	8	9.295E-22	-9.195E-09
9	2.244E-20	-9.582E-09	10	2.607E-21	-9.582E-09	11	-6.029E-20	-9.478E-09	12	4.213E-20	-9.478E-09
13	2.550E-18	-9.506E-09	14	1.391E-18	-9.506E-09	15	1.939E-18	-9.498E-09	16	2.790E-18	-9.498E-09
17	4.810E-18	-9.500E-09	18	2.951E-18	-9.500E-09	19	2.205E-18	-9.500E-09	20	2.977E-18	-9.500E-09
21	2.906E-18	-9.500E-09	22	5.554E-18	-9.500E-09	23	2.534E-19	-9.500E-09	24	-6.455E-19	-9.500E-09
25	8.612E-18	-9.500E-09	26	8.397E-18	-9.500E-09	27	6.971E-19	-9.500E-09	28	-6.456E-19	-9.500E-09
29	7.849E-18	-9.500E-09	30	7.621E-18	-9.500E-09	31	9.636E-18	-9.500E-09	32	9.177E-18	-9.500E-09
33	4.380E-18	-9.500E-09	34	4.503E-18	-9.500E-09	35	-1.064E-18	-9.500E-09	36	-1.109E-18	-9.500E-09

APPENDIX C. OUTPUT OF GENDVM TRANSPORT MODEL  
FOR THE COUPLED UNSATURATED-SATURATED FLOW SYSTEM AT YUCCA MOUNTAIN

Table I. Radionuclide Discharges to the Accessible Environment from GENDVM Coupled Saturated-Unsaturated Flow Model for Yucca Mountain.

RADIONUCLIDE DISCHARGE RATE (CI/DAY)							
YEAR	C14	HT59	SR90	TC99	U234	PU239	
1000.	0.	0.	0.	0.	0.	0.	
6730.	0.	0.	0.	0.	0.	0.	
12460.	0.	0.	0.	0.	0.	0.	
18190.	0.	0.	0.	0.	0.	0.	
23020.	0.	0.	0.	0.	0.	0.	
29650.	0.	0.	0.	0.	0.	0.	
35380.	0.	0.	0.	0.	0.	0.	
41110.	.11529E-08	.56134E-06	0.	0.	0.	0.	
46840.	.68404E-05	.48441E-02	0.	0.	0.	0.	
52570.	.29412E-05	.39530E-02	0.	0.	0.	0.	
58300.	.14684E-05	.37575E-02	0.	0.	0.	0.	
64030.	.73422E-06	.35756E-02	0.	0.	0.	0.	
69760.	.36711E-06	.34024E-02	0.	0.	0.	0.	
75490.	.18355E-06	.32376E-02	0.	0.	0.	0.	
81220.	.91777E-07	.30808E-02	0.	0.	0.	0.	
86950.	.45888E-07	.29316E-02	0.	0.	0.	0.	
92680.	.22944E-07	.27896E-02	0.	0.	0.	0.	
98410.	.11472E-07	.26545E-02	0.	0.	0.	0.	
104140.	.57361E-08	.25259E-02	0.	0.	0.	0.	
109870.	.28680E-08	.24035E-02	0.	0.	0.	0.	
115600.	.14340E-08	.22871E-02	0.	0.	0.	0.	
121330.	.71701E-09	.21764E-02	0.	0.	0.	0.	
127060.	.35850E-09	.20709E-02	0.	0.	0.	0.	
132790.	.17925E-09	.19706E-02	0.	0.	0.	0.	
138520.	.89620E-10	.18750E-02	0.	0.	0.	0.	
144250.	.12708E-10	.50297E-03	0.	0.	0.	0.	
149980.	.52574E-13	.28832E-05	0.	0.	0.	0.	
155710.	0.	0.	0.	0.	0.	0.	
161440.	0.	0.	0.	0.	0.	0.	
167170.	0.	0.	0.	0.	0.	0.	
172900.	0.	0.	0.	0.	0.	0.	
178630.	0.	0.	0.	0.	0.	0.	
184360.	0.	0.	0.	0.	0.	0.	
190090.	0.	0.	0.	0.	0.	0.	
195820.	0.	0.	0.	0.	0.	0.	
201550.	0.	0.	0.	0.	0.	0.	
207280.	0.	0.	0.	0.	0.	0.	
213010.	0.	0.	0.	0.	0.	0.	
218740.	0.	0.	0.	0.	0.	0.	
224470.	0.	0.	0.	0.	0.	0.	
230200.	0.	0.	0.	0.	0.	0.	
235930.	0.	0.	0.	0.	0.	0.	
241660.	0.	0.	0.	0.	0.	0.	
247390.	0.	0.	0.	0.	0.	0.	
253120.	0.	0.	0.	0.	0.	0.	
258850.	0.	0.	0.	0.	0.	0.	
264580.	0.	0.	0.	0.	0.	0.	
270310.	0.	0.	0.	0.	0.	0.	
276040.	0.	0.	0.	0.	0.	0.	
281770.	0.	0.	0.	0.	0.	0.	
287500.	0.	0.	0.	0.	0.	0.	
293230.	0.	0.	0.	0.	0.	0.	
298960.	0.	0.	0.	0.	0.	0.	
304690.	0.	0.	0.	0.	0.	0.	
310420.	0.	0.	0.	0.	0.	0.	
316150.	0.	0.	0.	0.	0.	0.	
321880.	0.	0.	0.	0.	0.	0.	
327610.	0.	0.	0.	0.	0.	0.	
333340.	0.	0.	0.	0.	0.	0.	
339070.	0.	0.	0.	0.	0.	0.	

Table I. (Continued).

RADIONUCLIDE DISCHARGE RATE (CI/DAY)							
YEAR	C14	NI59	SR90	TC99	U238	PU239	
688600.	0.	0.	0.	0.	0.	0.	0.
694330.	0.	0.	0.	0.	0.	0.	0.
700060.	0.	0.	0.	0.	0.	0.	0.
705790.	0.	0.	0.	0.	0.	0.	0.
711520.	0.	0.	0.	0.	0.	0.	0.
717250.	0.	0.	0.	0.	0.	0.	0.
722980.	0.	0.	0.	0.	0.	0.	0.
728710.	0.	0.	0.	0.	0.	0.	0.
734440.	0.	0.	0.	0.	0.	0.	0.
740170.	0.	0.	0.	0.	0.	0.	0.
745900.	0.	0.	0.	0.	0.	0.	0.
751630.	0.	0.	0.	0.	0.	0.	0.
757360.	0.	0.	0.	0.	0.	0.	0.
763090.	0.	0.	0.	0.	0.	0.	0.
768820.	0.	0.	0.	0.	0.	0.	0.
774550.	0.	0.	0.	0.	0.	0.	0.
780280.	0.	0.	0.	0.	0.	0.	0.
786010.	0.	0.	0.	0.	0.	0.	0.
791740.	0.	0.	0.	0.	0.	0.	0.
797470.	0.	0.	0.	0.	0.	0.	0.
803200.	0.	0.	0.	0.	0.	0.	0.
808930.	0.	0.	0.	0.	0.	0.	0.
814660.	0.	0.	0.	0.	0.	0.	0.
820390.	0.	0.	0.	0.	0.	0.	0.
826120.	0.	0.	0.	0.	0.	0.	0.
831850.	0.	0.	0.	0.	0.	0.	0.
837580.	0.	0.	0.	0.	0.	0.	0.
843310.	0.	0.	0.	0.	0.	0.	0.
849040.	0.	0.	0.	0.	0.	0.	0.
854770.	0.	0.	0.	0.	0.	0.	0.
860500.	0.	0.	0.	0.	0.	0.	0.
866230.	0.	0.	0.	0.	0.	0.	0.
871960.	0.	0.	0.	0.	0.	0.	0.
877690.	0.	0.	0.	0.	0.	0.	0.
883420.	0.	0.	0.	0.	0.	0.	0.
889150.	0.	0.	0.	0.	0.	0.	0.
894880.	0.	0.	0.	0.	0.	0.	0.
900610.	0.	0.	0.	0.	0.	0.	0.
906340.	0.	0.	0.	0.	0.	0.	0.
912070.	0.	0.	0.	0.	0.	0.	0.
917800.	0.	0.	0.	0.	0.	0.	0.
923530.	0.	0.	0.	0.	0.	0.	0.
929260.	0.	0.	0.	0.	0.	0.	0.
934990.	0.	0.	0.	0.	0.	0.	0.
940720.	0.	0.	0.	0.	0.	0.	0.
946450.	0.	0.	0.	0.	0.	0.	0.
952180.	0.	0.	0.	0.	0.	0.	0.
957910.	0.	0.	0.	0.	0.	0.	0.
963640.	0.	0.	0.	0.	0.	0.	0.
969370.	0.	0.	0.	0.	0.	0.	0.
975100.	0.	0.	0.	0.	0.	0.	0.
980830.	0.	0.	0.	0.	0.	0.	0.
986560.	0.	0.	0.	0.	0.	0.	0.
992290.	0.	0.	0.	0.	0.	0.	0.
998020.	0.	0.	0.	0.	0.	0.	0.
1003750.	0.	0.	0.	0.	0.	0.	0.
				.54941E-25	0.	0.	0.
				.1855AE-23	0.	0.	0.
				.52355E-22	0.	0.	0.
				.12444E-20	0.	0.	0.
				.25115E-19	0.	0.	0.
				.43359E-18	0.	0.	0.
				.64460E-17	0.	0.	0.
				.83035E-16	0.	0.	0.
				.93213E-15	0.	0.	0.
				.91673E-14	0.	0.	0.
				.79383E-13	0.	0.	0.
				.60804E-12	0.	0.	0.
				.41377E-11	0.	0.	0.
				.25117E-10	0.	0.	0.
				.13654E-09	0.	0.	0.
				.6670AE-09	0.	0.	0.
				.29394E-08	0.	0.	0.
				.11720E-07	0.	0.	0.
				.4241AE-07	0.	0.	0.
				.13979E-06	0.	0.	0.
				.42065E-06	0.	0.	0.
				.11593E-05	0.	0.	0.
				.79340E-05	0.	0.	0.
				.68386E-05	0.	0.	0.
				.14720E-04	0.	0.	0.
				.29340E-04	0.	0.	0.
				.54314E-04	0.	0.	0.
				.93652E-04	0.	0.	0.
				.1508AE-03	0.	0.	0.
				.2278AE-03	0.	0.	0.
				.32373E-03	0.	0.	0.
				.43432E-03	0.	0.	0.
				.55255E-03	0.	0.	0.
				.66966E-03	0.	0.	0.
				.77696E-03	0.	0.	0.
				.86757E-03	0.	0.	0.
				.9375AE-03	0.	0.	0.
				.98605E-03	0.	0.	0.
				.1014AE-02	0.	0.	0.
				.10270E-02	0.	0.	0.
				.10259E-02	0.	0.	0.
				.10143E-02	0.	0.	0.
				.9935AE-03	0.	0.	0.
				.96353E-03	0.	0.	0.